eLIFE
elifesciences.org

RESEARCH ARTICLE

Figures and figure supplements

Nitric oxide radicals are emitted by wasp eggs to kill mold fungi

Erhard Strohm *et al*

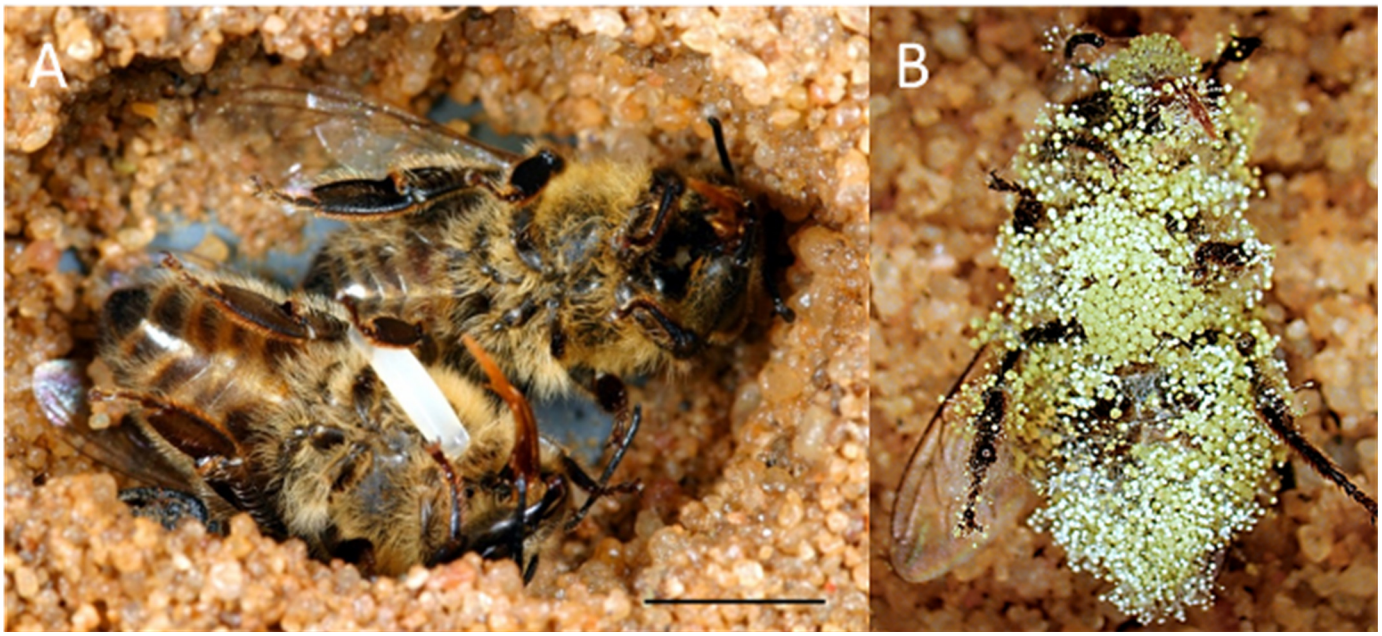

Figure 1. Paralyzed honeybees under different conditions. (**A**) Brood cell of the European beewolf with two bees, one carrying an egg, in an observation cage. (**B**) Honeybee paralyzed by a beewolf female but immediately removed and kept in an artificial brood cell, heavily overgrown by mold fungi that have already developed conidia. Scale bar = 5 mm.

DOI: https://doi.org/10.7554/eLife.43718.003

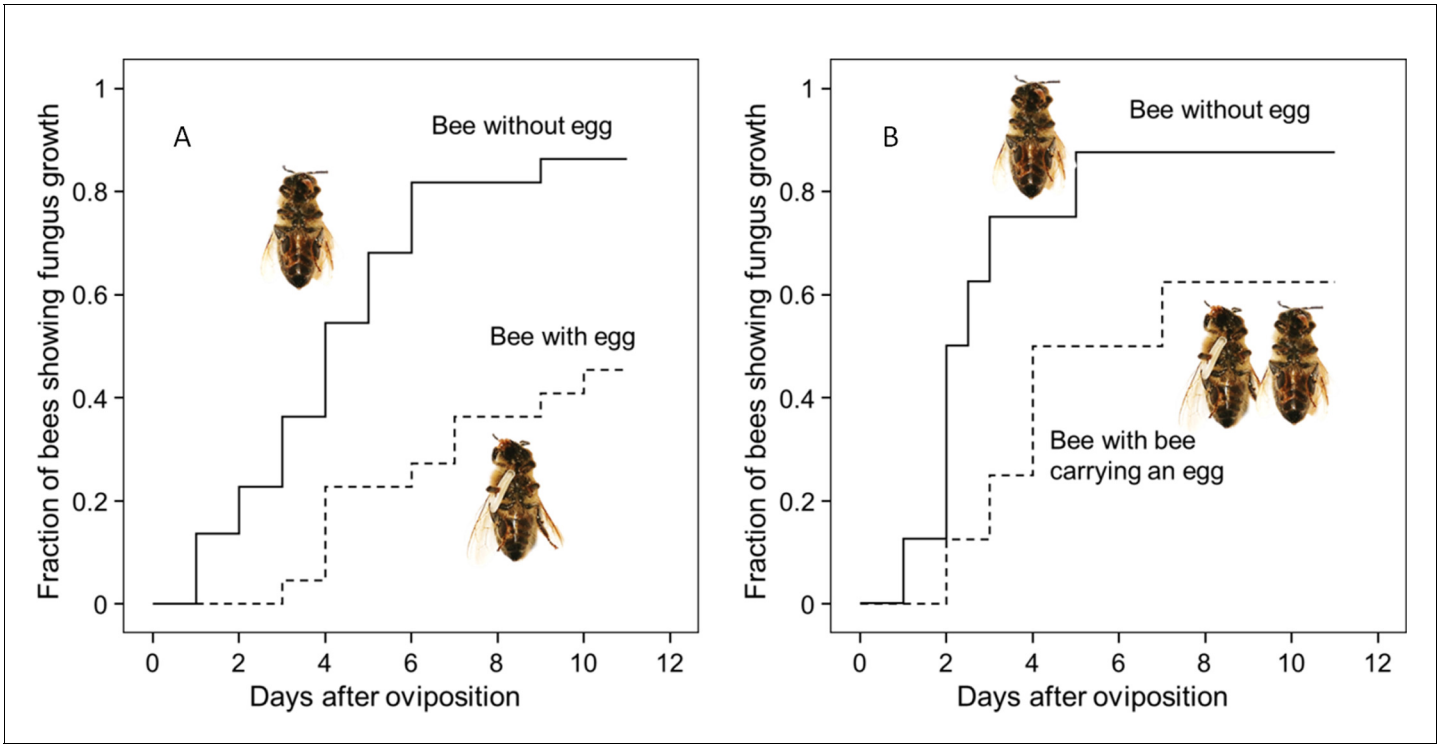

Figure 2. Onset of fungal growth on paralyzed honeybees taken from *Philanthus triangulum* nests and kept in artificial brood cells. The fraction of bees showing first signs of fungal growth is shown as a function of days since oviposition. (**A**) Honeybees that either carried an egg (dashed line) or not (solid line) (N = 22 each, hazard ratio = 0.29, 95% confidence interval: 0.13–0.64). (**B**) Honeybees that were either kept alone (solid line) or shared a brood cell with a bee carrying an egg (dashed line) (N = 16 each, hazard ratio = 0.39, 95% confidence interval: 0.17–0.9).

DOI: https://doi.org/10.7554/eLife.43718.004

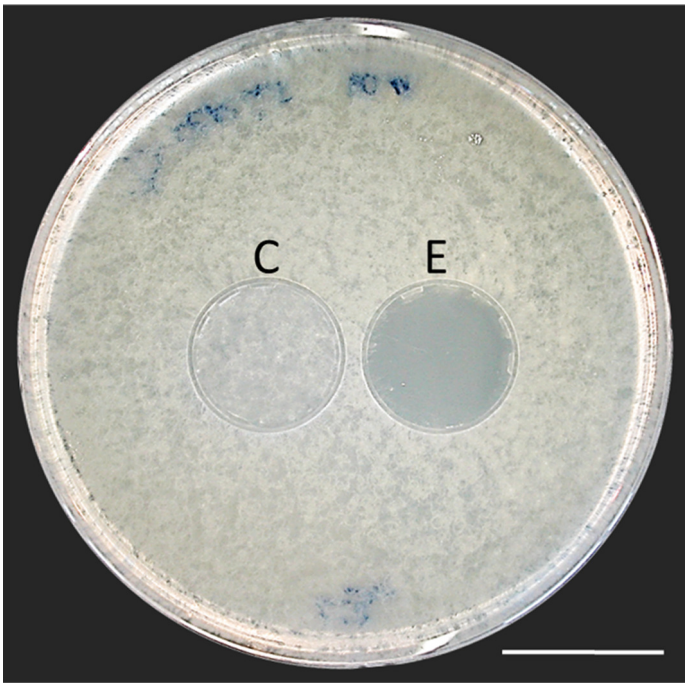

Figure 3. Bioassay demonstrating the inhibitory effect of a beewolf egg against *Aspergillus flavus*. Two areas on the agar were covered by caps of a volume similar to natural beewolf brood cells. One cap, the control (**C**), was empty, while the experimental cap (**E**) contained a fresh beewolf egg attached to the ceiling of the cap. The caps were removed and the picture was taken after 24 hr of incubation at 25°C. The control area (**C**) shows dense whitish fungal hyphae similar to the surroundings. However, the area that was exposed to the volatiles from a beewolf egg (**E**) shows bare agar, indicating that the growth of this aggressive fungus was entirely inhibited. Scale bar = 2.5 cm.

DOI: https://doi.org/10.7554/eLife.43718.006

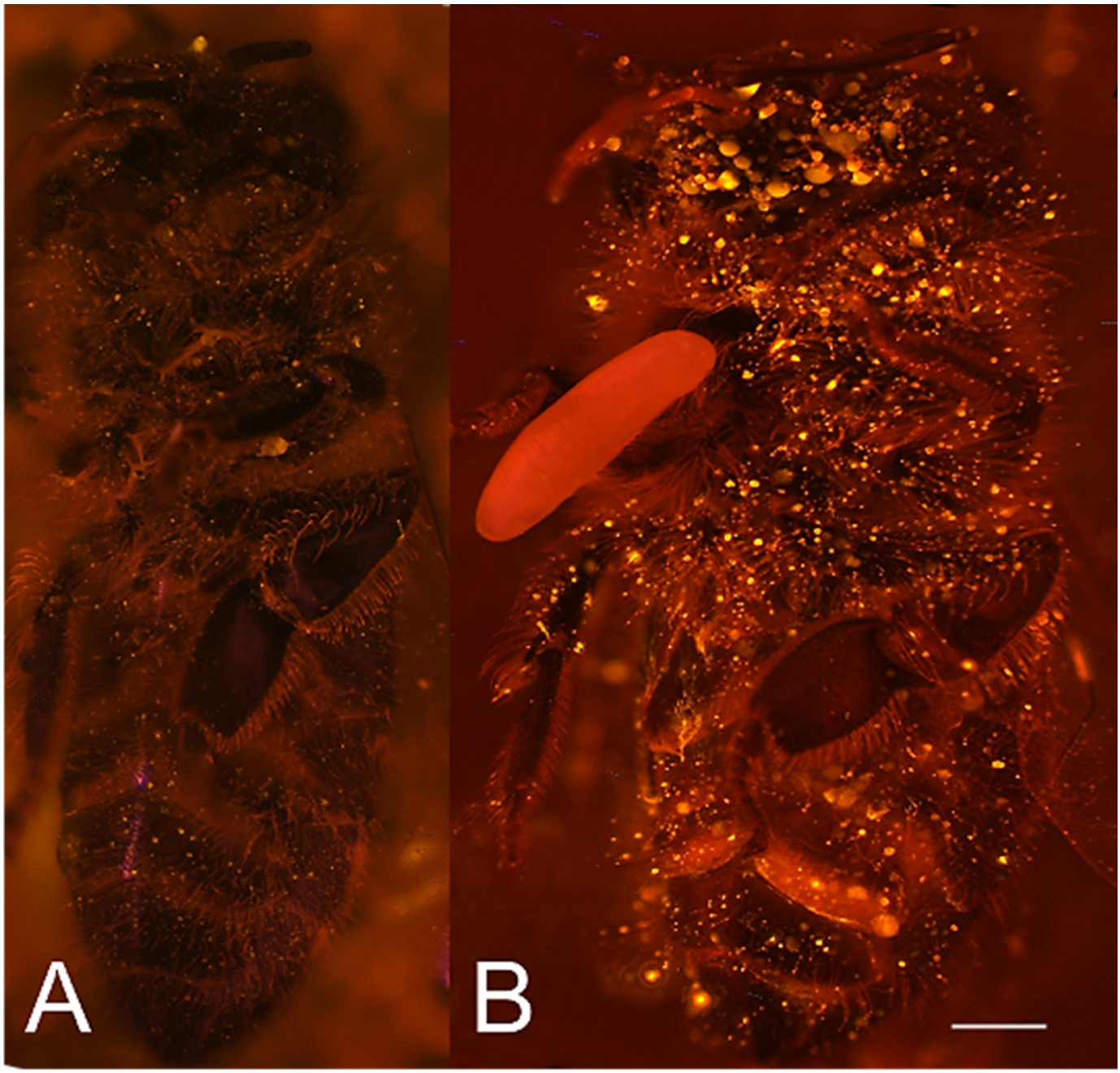

Figure 4. Visualization of NO˙ emission by beewolf eggs using fluorescence imaging. (**A**) Honeybee from a brood cell without an egg and (**B**) honeybee with egg. Both bees were sprayed with a solution of the NO˙ specific fluorescence probe DAR4M-AM. Only the droplets on the bee with the egg (**B**) show a bright yellow and orange fluorescence indicating the presence of NO˙. Images are composites of multiple pictures of the x/y plane and z-axis. Scale bar = 1 mm.

DOI: https://doi.org/10.7554/eLife.43718.007

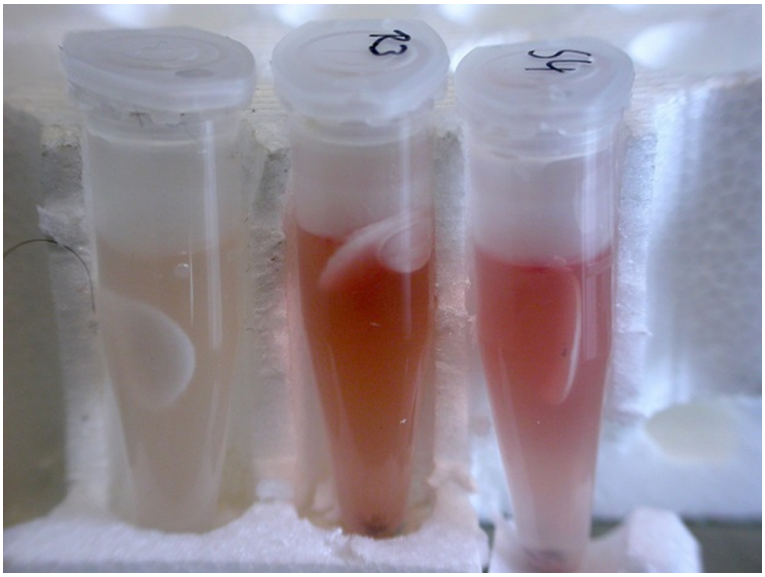

Figure 4—figure supplement 1. Results of the Griess assay with beewolf eggs. The left reaction vial is a control without beewolf egg, the other two vials containd eggs that were placed in the lid within 1 hr of oviposition. Vials were incubated at 25°C for 24 hr.

DOI: https://doi.org/10.7554/eLife.43718.008

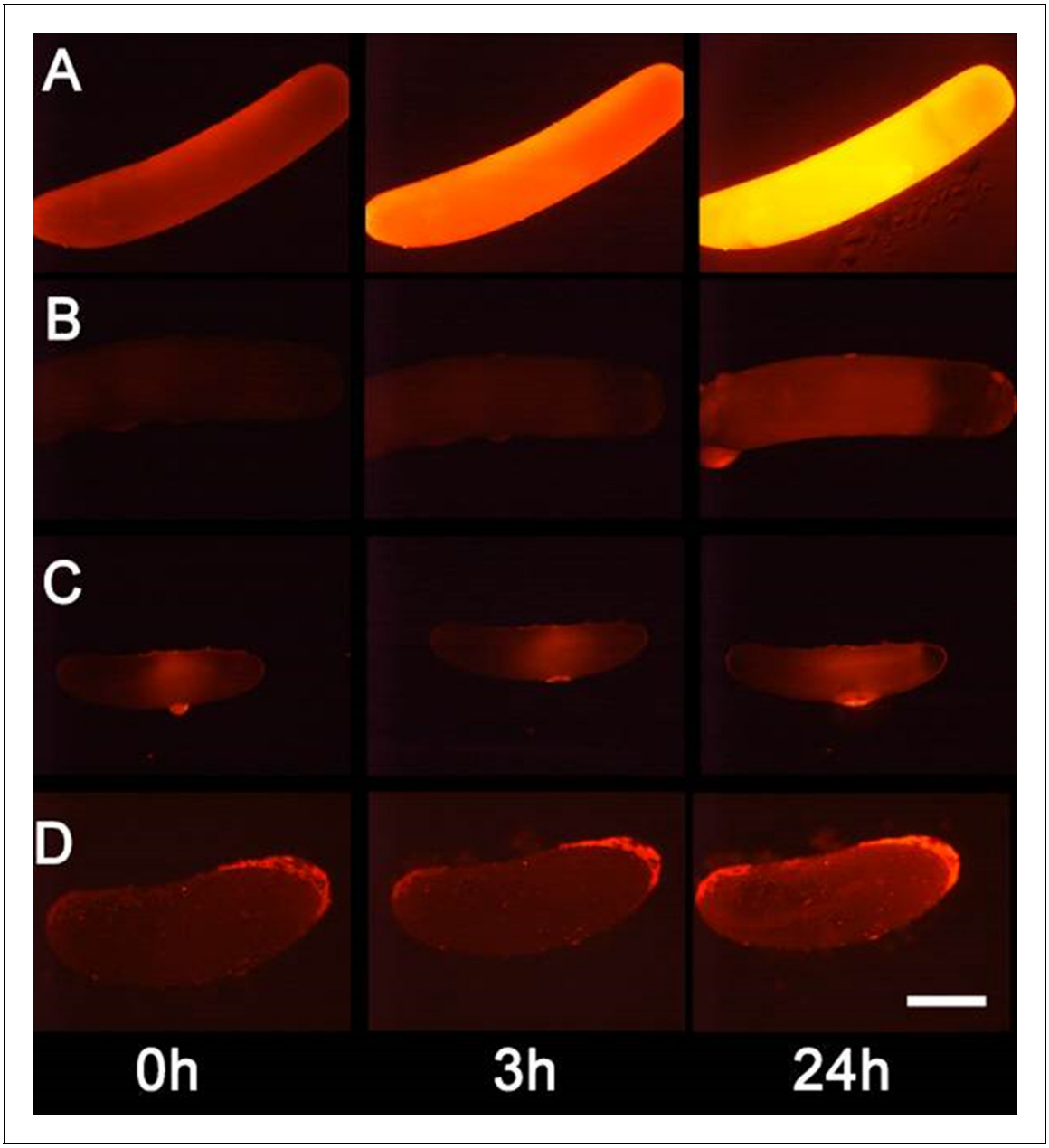

Figure 5. Detection of nitric oxide ($NO^{\cdot}$) in beewolf eggs. Newly laid eggs of beewolves, *Philanthus triangulum*, of the cockroach wasp *Ampulex compressa* and of the Red Mason bee, *Osmia bicornis* were injected with the $NO^{\cdot}$ sensitive fluorescence probe DAR4M-AM. Control beewolf eggs were injected with phosphate buffer. Images were obtained by fluorescence microscopy 0, 3 and 24 hr after injection. Row (**A**) DAR4M-AM injected beewolf egg showing strong increase in fluorescence; (**B**) Buffer-injected control beewolf egg showing the level of autofluorescence; (**C**) DAR4M-AM injected egg of *A. compressa;* (**D**) DAR4M-AM injected egg of *O. bicornis*. Scale bar: 1 mm.

DOI: https://doi.org/10.7554/eLife.43718.009

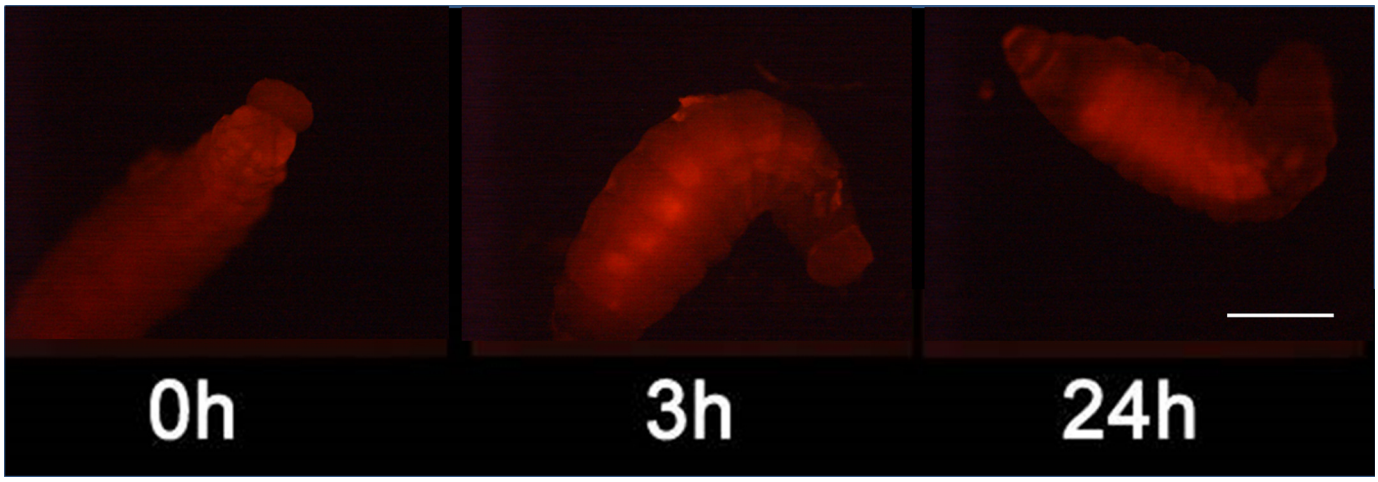

Figure 5—figure supplement 1. Detection of nitric oxide ($NO^{\cdot}$) in beewolf larva. Newly hatched beewolf larva, *Philanthus triangulum*, was injected with the $NO^{\cdot}$ sensitive fluorescence probe DAR4M-AM. Images were obtained by fluorescence microscopy 0, 3 and 24 hr after injection. Scale bar: 1 mm.
DOI: https://doi.org/10.7554/eLife.43718.010

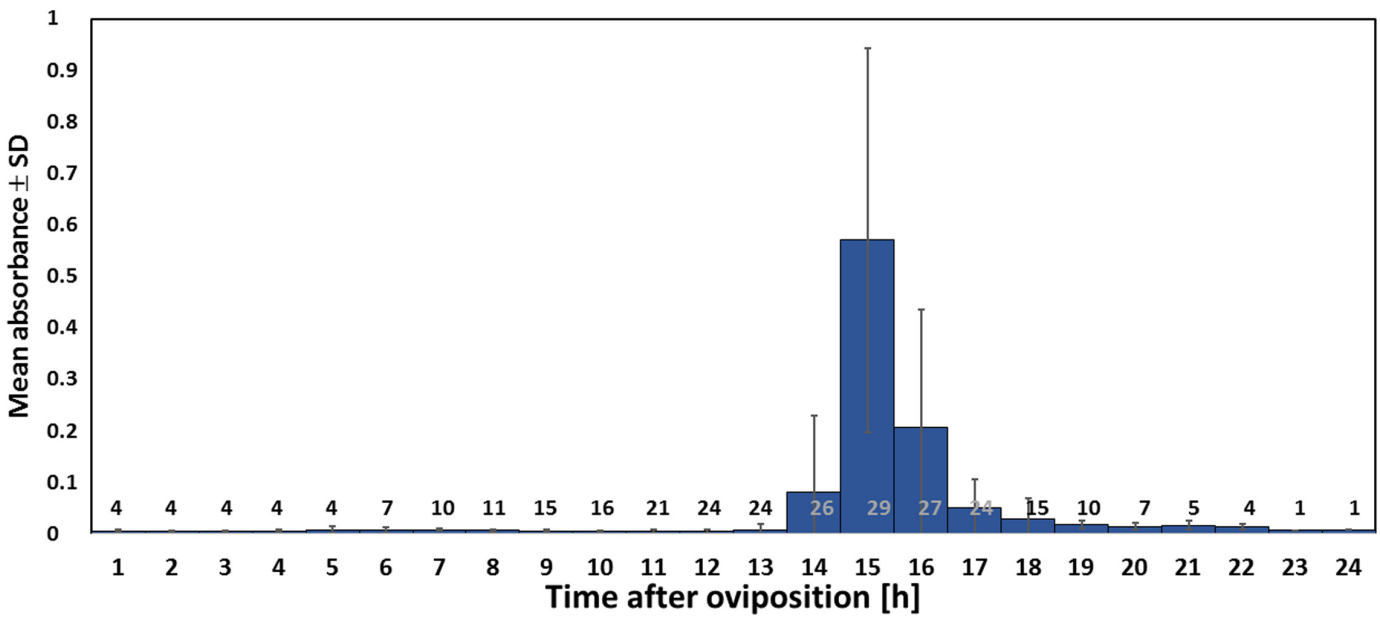

Figure 6. Timing of NO· emission from beewolf eggs (kept at 28°C). The photometrically determined absorbance at 590 nm (mean ± SD) is shown as a function of time after oviposition for iodide-starch solutions successively exposed to beewolf eggs for one hour. Sample size (number of eggs measured) at each one hour interval is indicated above the x-axis.

DOI: https://doi.org/10.7554/eLife.43718.012

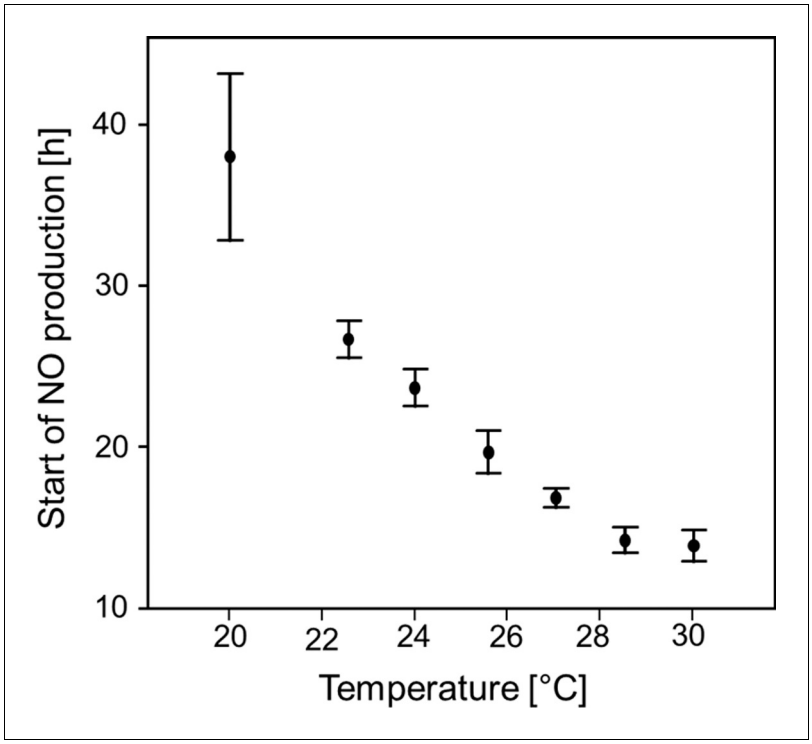

Figure 6—figure supplement 1. Start of NO˙ emission (h after oviposition) as a function of temperature. Beewolf eggs were kept at different temperatures and the onset of NO˙ release was assessed using the color change of an iodide starch solution as monitored by a digital camera at 30 min intervals. Symbols are means ± SD (Quadratic regression: R^2 = 0.98, N = 33, p<0.001; Q_{10} = 2.74). Source data file: ***Figure 6—figure supplement 1—source data 1***.

DOI: https://doi.org/10.7554/eLife.43718.013

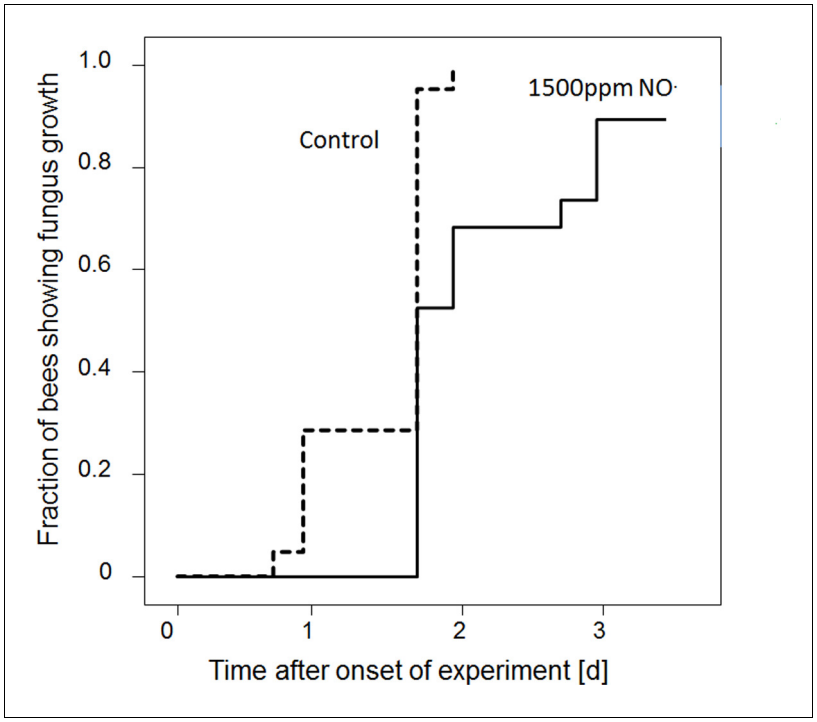

Figure 7. Onset of fungal growth (time after onset of experiment) on honeybees that were not embalmed in artificial brood cells. Brood cells were either injected with synthetic NO· to a concentration of 1500ppm (solid line) or were injected with nitrogen (dashed line) (N = 20 each, hazard ratio = 0.41, 95% confidence interval: 0.198–0.845).

DOI: https://doi.org/10.7554/eLife.43718.016

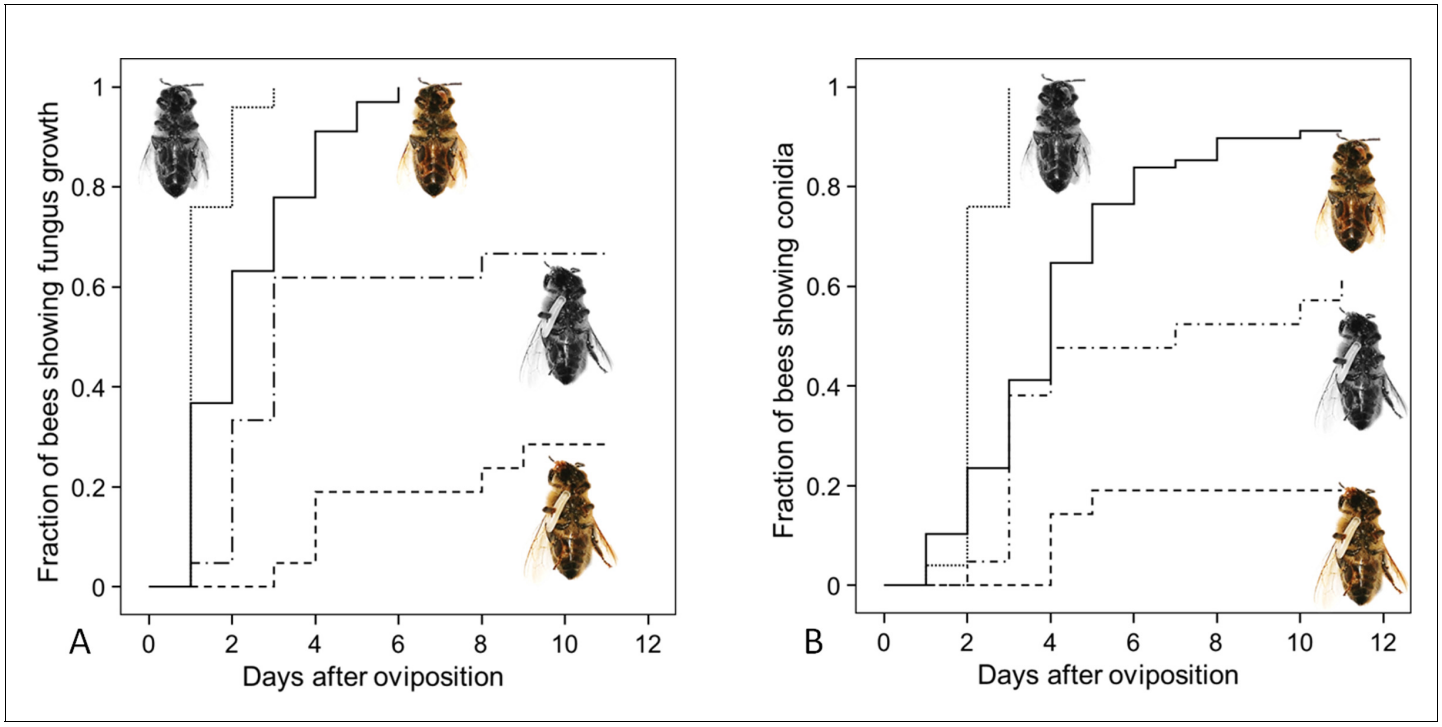

Figure 8. Fungus growth on honeybees of four different treament groups. Timing of occurrence of (**A**) fungal hyphae and (**B**) conidia on paralyzed honeybees that were (1) not embalmed by beewolf females and did not carry an egg (n = 25, colorless bee, point line), (2) embalmed but did not carry an egg (n = 68, colored bee, solid line), (3) not embalmed but carried an egg (n = 21, colorless bee with egg, dash-point line) or (4) embalmed and carried an egg (n = 21, colored bee with egg, dashed line). See ***Appendix 1—table 2*** for hazard ratios.

DOI: https://doi.org/10.7554/eLife.43718.018

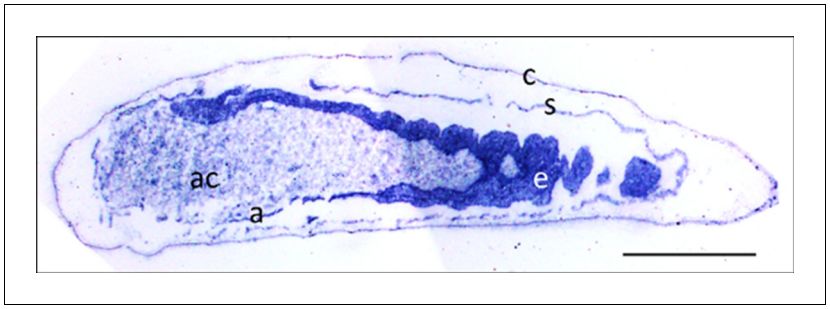

Figure 9. Micrograph of a longitudinal section of a beewolf egg fixed 15–16 hr after oviposition showing fixation insensitive NADPH-diaphorase activity. Strong blue staining in the embryonic tissue indicates the presence of reduced nitroblue tetrazolium demonstrating NOS activity (c = cuticle, s = serosa, e = embryo, a = amnion, ac = amnion cavity, scale bar = 1 mm, image composed from two separate photos of the left and right parts of the egg.).

DOI: https://doi.org/10.7554/eLife.43718.020

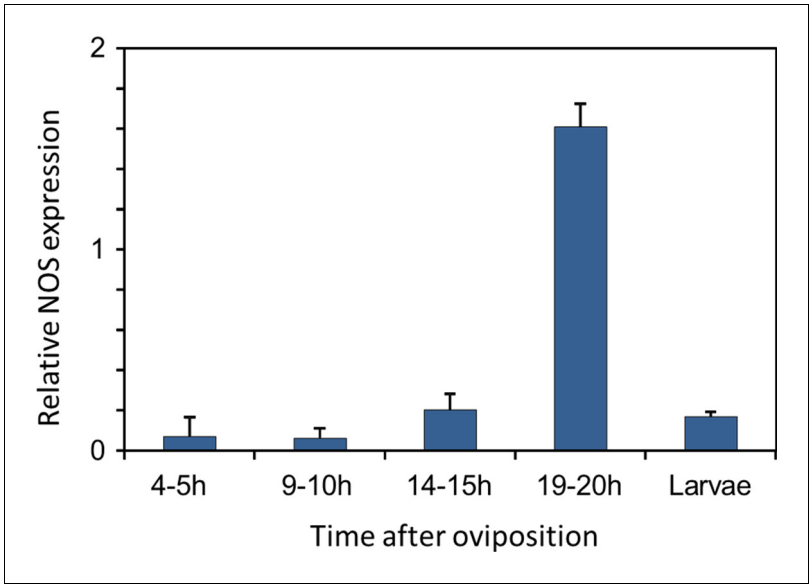

Figure 10. Gene expression of NOS relative to ß-actin in beewolf eggs at different times after oviposition and in freshly hatched larvae. Two trials were conducted, each with 25 pooled eggs or larvae per time interval. Mean ratios of NOS-mRNA to ß-Actin-mRNA are shown (with standard deviations), as determined by Q-RT-PCR.
DOI: https://doi.org/10.7554/eLife.43718.021

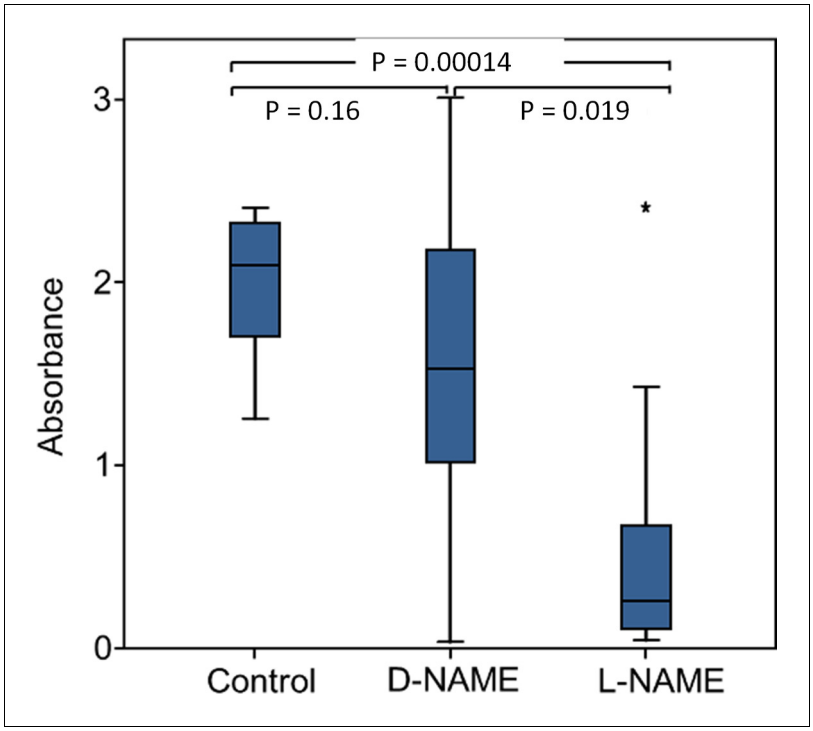

Figure 11. Effect of NOS inhibition on $NO^{\cdot}$ production. Amount of $NO^{\cdot}$ and/or $NO_2^{\cdot}$ emanating from non-injected beewolf eggs (control; N = 14) and those injected with D-NAME (a non-inhibiting enantiomer of L-NAME, N = 9) or L-NAME (a NOS inhibiting L-arginine analog, N = 14). The photometrically determined absorbance at 590 nm is shown for iodide-starch solutions that were exposed for 24 hr to the headspace of eggs of the indicated treatment group (shown are median, quartiles and range, * indicates an outlier, included in the analysis). P-values are for Holm-corrected Mann-Whitney U-tests.

DOI: https://doi.org/10.7554/eLife.43718.023

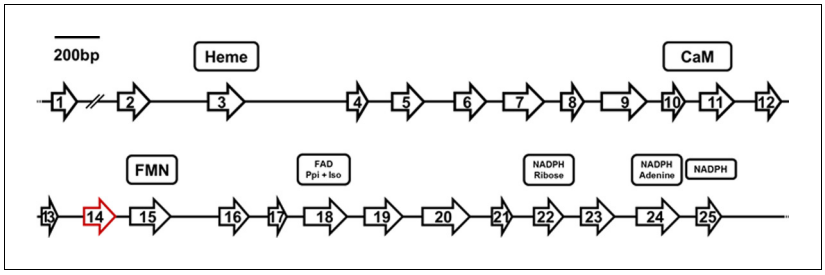

Figure 11—figure supplement 1. Structure of the *Pt-NOS* gene indicating position and length of exons. Exon 14 (red) is missing in the NOS mRNA in beewolf eggs compared to adults. Presumed cofactor-binding domains as deduced from homologous sequences of the *NOS* of *Anopheles stephensi* (***Luckhart et al., 1998***; ***Luckhart and Li, 2001***) are indicated for heme, calmodulin (CaM), FMN, FAD pyrophosphate (FAD PPi) and FAD isoalloxazine (FAD Iso), NADPH ribose, NADPH adenine, and NADPH.

DOI: https://doi.org/10.7554/eLife.43718.024

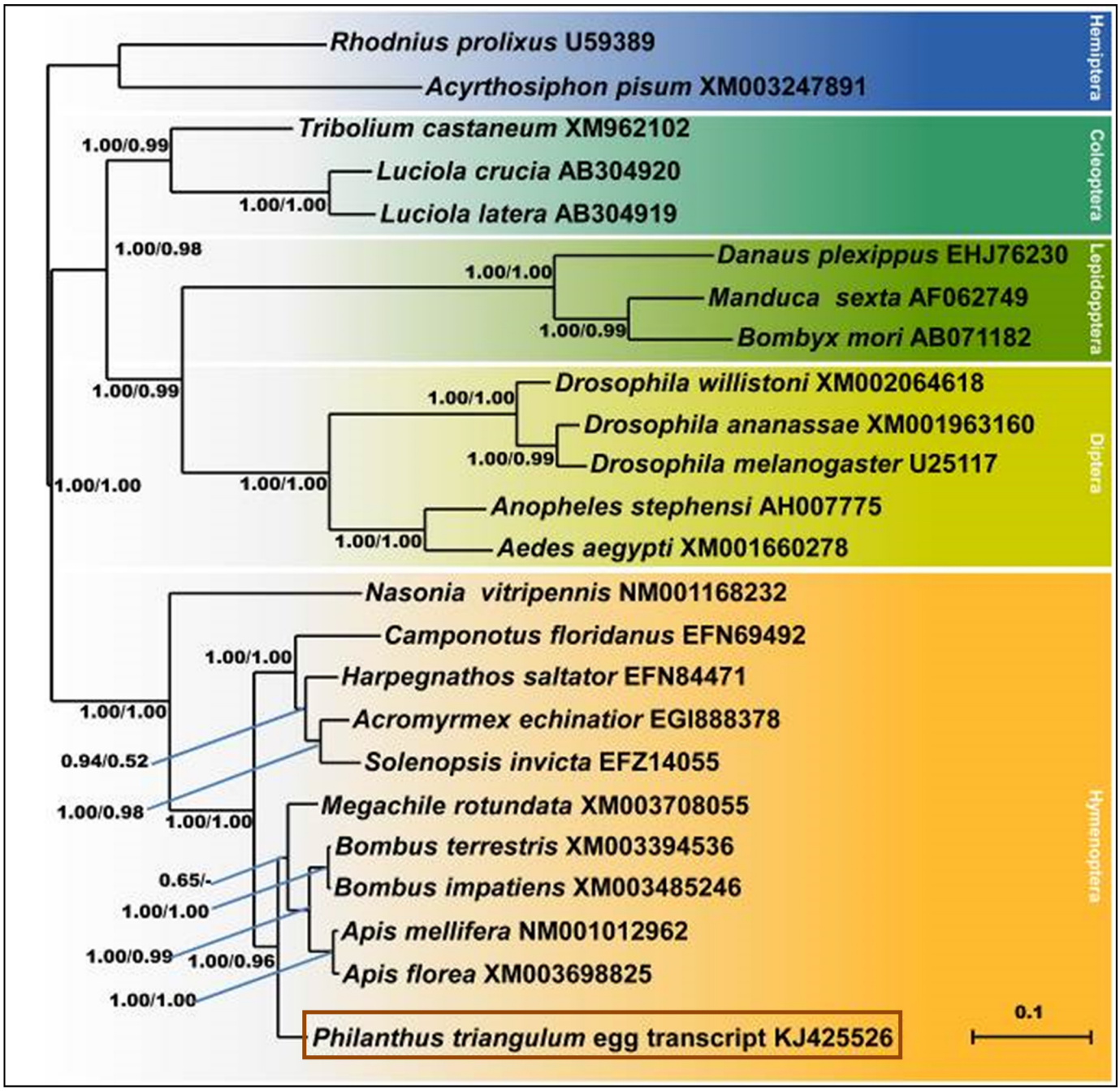

Figure 11—figure supplement 2. Consensus tree obtained from Bayesian analysis of NOS amino acid sequences from five orders of insects (distinguished by different colors), including the NOS sequences of *P. triangulum* eggs (lowermost entry). Values at the nodes represent Bayesian posterior probabilities and local support values (FastTree analysis), respectively. Scale bar represents 0.1 changes per site.

DOI: https://doi.org/10.7554/eLife.43718.025